Quantum Langevin model for nonequilibrium condensation

Alessio Chiocchetta
SISSA - International School for Advanced Studies, via Bonomea 265, 34136 Trieste, Italy
and INFN - Istituto Nazionale di Fisica Nucleare, Sezione di Trieste, Italy

Iacopo Carusotto
INO-CNR BEC Center and Dipartimento di Fisica, Università di Trento, Via Sommarive 14, I-38123 Povo, Italy
(Received 3 June 2014; published 28 August 2014)

We develop a quantum model for nonequilibrium Bose-Einstein condensation of photons and polaritons in planar microcavity devices. The model builds on laser theory and includes the spatial dynamics of the cavity field, a saturation mechanism, and some frequency dependence of the gain: quantum Langevin equations are written for a cavity field coupled to a continuous distribution of externally pumped two-level emitters with a well-defined frequency. As an example of application, the method is used to study the linearized quantum fluctuations around a steady-state condensed state. In the good-cavity regime, an effective equation for the cavity field only is proposed in terms of a stochastic Gross-Pitaevskii equation. Perspectives in view of a full quantum simulation of the nonequilibrium condensation process are finally sketched.

DOI: 10.1103/PhysRevA.90.023633 PACS number(s): 03.75.Kk, 05.70.Ln, 71.36.+c

I. INTRODUCTION

Recent experimental demonstrations of Bose-Einstein condensation (BEC) phenomena in luminous gases of exciton-polaritons [1–4] and pure photons [5] in optical microcavities are opening exciting new perspectives to the study of nonequilibrium statistical mechanics of open, driven-dissipative systems. In contrast to the usual statistical mechanics where the equilibrium density matrix is determined by the Boltzmann factor $\rho_{\text{eq}} \propto \exp(-H/k_B T)$, the steady state of open systems is determined by a dynamical balance of pumping and losses. The novel features that stem from this difference are presently attracting a lot of interest from both theoretical and experimental points of view, in particular for what concerns phase transitions and critical behavior [6–8].

In optics, the first and most celebrated example of phase transition is the laser operation threshold and its interpretation in terms of a spontaneously broken U(1) phase symmetry was first pointed out in the early 1970s [9–11]. While this analogy with Bose-Einstein condensation (BEC) is typically discussed in textbooks for the case of single-mode laser cavities, rigorously speaking the concepts of phase transition and of the spontaneous symmetry breaking phenomenon are restricted to spatially infinite systems. Only recently, the advances in optical technology are providing examples of spatially extended laser devices for which the large system limit is a legitimate approximation, the so-called VCSELs (vertical cavity surface emitting lasers) [12]. While these devices have received a great deal of attention from the point of view of nonlinear optics and of all-optical information processing [13], their potential to study the nonequilibrium statistical mechanics of the laser phase transition has been so far only marginally exploited [14].

As is reviewed in [15], the interest for these condensation phenomena in optical systems was strongly revived in the last decade with the experimental observations of polariton and photon BECs [1,2,4,5]. As a remarkable difference from standard lasers, it was pointed out that the effective interactions between the individual particles forming the photon and polariton gases mediated by the underlying medium may lead to collective behaviors in the gas including, e.g., superfluidity [16].

At the same time, significant work has been devoted to characterizing the equilibrium versus nonequilibrium nature of these condensates and quantifying the observable consequences of the pumping and loss processes. On one hand, the photon BEC experiment of [5] has shown clear evidence of a thermal Bose-Einstein distribution at the temperature of the cavity medium embedding the dye molecules. On the other hand, qualitatively novel features of nonequilibrium BEC have been observed in polariton condensation experiments. For example, the early experiments of [17] have shown BEC into a ring of modes at finite **k**: An interpretation of this effect in terms of an interplay of driving, dissipation, and energy minimization was proposed in [18] and experimentally confirmed by [19]. Another, even more surprising feature was experimentally reported in [20], where a thermal-like distribution was observed even in a weak-coupling regime where collisions are expected to be too weak to allow for any thermalization.

From the theoretical point of view, the recent work [21] has quantitatively explored the crossover from the equilibrium-like regime of [5] where the particle distribution closely follows the Bose-Einstein distribution, to nonequilibrium regimes where the distribution is more and more distorted up to the standard laser regime: in particular, the ratio between the thermalization rate (encoded by the absorption and emission rates) and the pumping and photon losses was identified as the key parameter determining the equilibrium versus nonequilibrium nature of the momentum distribution of photons.

Going beyond the one-body distribution function, several authors [22–24] have pointed out a qualitative signature of nonequilibrium in the dispersion of the collective excitations: the typical acoustic branch of equilibrium condensates is replaced by a diffusive plateau at low wave vectors, whose **k**-space extension is quantitatively related to the departure from equilibrium. Furthermore, the nonperturbative functional renormalization group calculation in [25] showed the importance of new critical exponents arising from the genuine nonequilibrium nature of the system. Finally, theoretical descriptions of the photon BEC phenomenon in purely laser terms were aimed for in [26]. An interesting proposal to obtain a chemical potential for photons was proposed in [27].

The situation is even more intriguing in the reduced-dimensions case that is naturally realized in experiments: While a well-developed condensate with spatial coherence extending in the whole gas was observed in the relatively small systems of [4,5], quasicondensation features are expected to arise in larger systems because of long-wavelength fluctuations. In the equilibrium case, the well-known Mermin-Wagner theorem forbids BEC in translationally invariant systems [28] of dimension smaller or equal to 2 [29]. In the nonequilibrium case, first theoretical works based on a Gaussian linearized theory of fluctuations have anticipated that the long-distance behavior of the nonequilibrium (interacting) quasicondensate should be the same as in the corresponding equilibrium system at finite T, that is an exponential decay of coherence in one dimension and a power-law decay in two dimensions [22,23,30]. Pioneering experiments along these lines were reported in [31,32]. Very recently, more refined theoretical studies going beyond the Gaussian theory have started questioning some aspects of these theoretical predictions. In particular, it was pointed out in [33,34] that terms beyond the linearized Bogoliubov theory are essential to correctly capture the long-distance behavior of the spatial coherence and correct some pathologies found in the noninteracting limit in [30]. As a result, the power-law quasi-long-range order of spatially homogeneous two-dimensional quasicondensates might be broken and replaced by a stretched exponential decay [33].

The common starting point of all these theoretical works is phenomenological stochastic Gross-Pitaevskii equations (SGPE). The only exception is the numerical simulation reported in [35] where the BEC phase transition was studied in the so-called optical parametric oscillator (OPO) configuration which is amenable to an almost *ab initio* truncated-Wigner description of the field dynamics. In all other cases, the strength and the functional form of the noise terms had to be introduced in a phenomenological way [30,36]. The purpose of this work is to develop a fully quantum model of the system from which one can derive a SGPE under controlled approximations. In contrast to previous derivations of the SGPE based, e.g., on Keldysh formalism [37] or on the truncated-Wigner representations of the field [35,36], our derivation is performed through the quantum Langevin approach [38]: on one hand, this approach offers a physically transparent description of the baths and, in particular, of the incoherent pumping mechanism. On the other hand, it allows us to capture within a simple Markovian theory the frequency dependence of the pumping and dissipation baths. In the good-cavity limit, we can then adiabatically eliminate the matter degrees of freedom, which results in an effective dynamics for the cavity photon field only: in particular, explicit expressions for the Langevin terms are provided, which can eventually be used as a starting point for more sophisticated statistical mechanics calculations.

This article is organized as follows. In Sec. II we present the model and we derive the quantum Langevin equations. In Sec. III, we present the mean-field theory of the condensation process and we illustrate the U(1) spontaneous symmetry breaking phenomenon. In the following Sec. IV we study the excitation modes of the system and the effect of fluctuations around the condensate; in particular, predictions for the momentum distribution of the thermal component and for the luminescence spectrum are given. In Sec. V we discuss the good-cavity limit where our equations can be reduced to a stochastic Gross-Pitaevskii equation. Conclusions are finally drawn in Sec. VI.

II. THE MODEL

Our microscopic theory extends early models on laser operation [39–42] to the spatially extended case of planar cavities with a parabolic dispersion of the cavity photon as a function of the in-plane wave vector $\mathbf{k}$,

$$\omega_{\mathbf{k}} = \omega_0 + \frac{k^2}{2m}, \tag{1}$$

with a cutoff frequency ω_0 and an effective mass m [15]. This simple description of cavity modes well captures the physics of planar DBR semiconductor microcavities in both the weak and the strong light-matter coupling regimes: in particular, low-momentum polaritons used in the condensation experiment [4] are straightforwardly included as dressed photon modes with suitably renormalized ω_0 and m parameters. When supplemented with a harmonic potential term accounting for the mirror curvature, this same formalism also describes the mesoscopic cavity of [5].

As is sketched in Fig. 1, the cavity field is then coupled to a set of two-level emitters. Both the emitters and the cavity are subject to losses of different natures, while energy is continuously injected into the system by pumping the emitters to their excited state. The steady state of the system is therefore determined by a dynamical balance of pumping and losses. In this description, both Bose-Einstein condensation and lasing consist in the appearance of a macroscopic coherent field in a single mode of the cavity (typically the $\mathbf{k} = 0$ one), monochromatically oscillating at a given frequency ω and with a long-distance coherence extending in the whole system. Part of the in-cavity light eventually leaves the cavity via the nonperfectly reflecting mirror and ends up forming a coherent output beam of light.

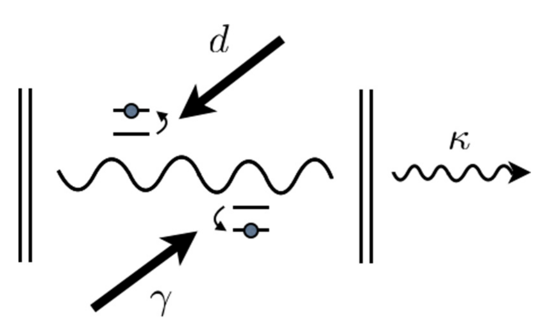

FIG. 1. (Color online) A pictorial representation of the model. Emitters lose energy at a rate γ while energy is pumped in at a rate d. Photons can leave the cavity after a time κ^{-1}.

While this theory directly builds on standard laser theory, it is generic enough to capture the main specificities of exciton-polariton condensation under an incoherent pumping scheme which was experimentally demonstrated in [4]. In this case, the dispersion is the polariton one and the two-level emitters provide a model description of the complex irreversible polariton scattering processes replenishing the condensate [43,44]. The main gain process consists of binary polariton scattering where two polaritons located around the inflection point of their dispersion are scattered into one condensate polariton and one exciton (which is then quickly lost). In our model, the excited state of the emitters correspond to pairs of polaritons located around the inflection point of their dispersion, while the ground state of the emitter corresponds to having one exciton resulting from the collision. At simplest order, the emitter energy ν is then approximately equal to the difference of the energy of the pair around the inflection point and of the exciton, $\hbar\nu \approx 2E_{\text{infl}} - E_{\text{exc}}$, that is the energy where the collisional gain is expected to be maximum. Extensions of this theory including more complicate emitters can be used to describe the dye molecules involved in the photon condensation experiments of [5]. Several possibilities in this direction are explored in [21,45].

A. The field and emitter Hamiltonians and the radiation-emitter coupling

Given the translational symmetry of the system along the cavity plane, the in-plane momentum $\mathbf{k}$ of the photon is a good quantum number and the (bare) photon dispersion of a given longitudinal mode is well described by the parabolic dispersion (1). The emitters are fixed in space according to a regular square lattice and do not have any direct interaction.

Taking for notational simplicity $\hbar = 1$, the free Hamiltonian of the field and of the emitters has the usual form

$$H_{\text{free}} = \sum_{\mathbf{k}} \omega_{\mathbf{k}} b^\dagger_{\mathbf{k}} b_{\mathbf{k}} + \sum_i \nu S^z_i, \tag{2}$$

where $\omega_{\mathbf{k}}$ is the cavity dispersion defined in (1) and ν is the emitter frequency. The $b_{\mathbf{k}}, b^\dagger_{\mathbf{k}}$ operators satisfy bosonic commutation rules $[b_{\mathbf{k}}, b^\dagger_{\mathbf{k}'}] = \delta_{\mathbf{k},\mathbf{k}'}$, while the emitter operators $S^{\pm,z}$ satisfy the usual algebra of spin-1/2 operators.

Within the usual rotating-wave approximation, the radiation-matter coupling is then

$$H_{\text{int}} = \frac{ig}{\sqrt{V}} \sum_i \sum_{\mathbf{k}} \left(e^{i\mathbf{k}\cdot\mathbf{x}_i}\, b_{\mathbf{k}}\, S^+_i - e^{-i\mathbf{k}\cdot\mathbf{x}_i}\, b^\dagger_{\mathbf{k}}\, S^-_i\right), \tag{3}$$

where $\mathbf{x}_i$ is the position of the ith emitter and V is the total volume of the system.

Assuming periodic boundary conditions, we can introduce the D-dimensional real-space cavity field

$$\phi(\mathbf{x}) = \frac{1}{\sqrt{V}} \sum_{\mathbf{k}} e^{i\mathbf{k}\cdot\mathbf{x}}\, b_{\mathbf{k}}. \tag{4}$$

In terms of the field $\phi(\mathbf{x})$, local binary interactions between the cavity photons can be added to the model via a two-body interaction term of the form

$$H^{(4)} = \frac{\lambda}{2} \int_V d^D x\, \phi^\dagger(\mathbf{x})\phi^\dagger(\mathbf{x})\phi(\mathbf{x})\phi(\mathbf{x}), \tag{5}$$

which in momentum space reads

$$H^{(4)} = \frac{\lambda}{2V} \sum_{\mathbf{k}\mathbf{k}'\mathbf{q}} b^\dagger_{\mathbf{k}+\mathbf{q}} b^\dagger_{\mathbf{k}'-\mathbf{q}} b_{\mathbf{k}'} b_{\mathbf{k}}. \tag{6}$$

Physically, such a term can describe a Kerr $\chi^{(3)}$ optical nonlinearity of the cavity material or, equivalently, polariton-polariton interactions [15].

B. Dissipative field dynamics: Radiative losses

The cavity field is coupled to an external bath of radiative modes via the nonperfectly reflecting cavity mirrors. As usual, this can be modeled by coupling each $\mathbf{k}$ mode of the field with a bath of harmonic oscillators [46]. The resulting quantum Langevin equations [38] then have the form

$$\frac{db^\dagger_{\mathbf{k}}}{dt} = \left(i\omega_{\mathbf{k}} - \frac{\kappa}{2}\right) b^\dagger_{\mathbf{k}} + F^\dagger_{\mathbf{k}}. \tag{7}$$

Here, κ is the decay rate of the field and the zero-mean quantum noises $F^\dagger_{\mathbf{k}}$ are uncorrelated and have a delta-like correlation in time:

$$\langle F^\dagger_{\mathbf{k}}(t) F_{\mathbf{k}'}(t')\rangle = 0, \tag{8}$$

$$\langle F_{\mathbf{k}}(t) F^\dagger_{\mathbf{k}'}(t')\rangle = \kappa\, \delta(t - t')\, \delta_{\mathbf{k},\mathbf{k}'}. \tag{9}$$

This form of the quantum Langevin equation requires that the initial total density matrix factorize in the cavity and bath parts and that the bath density matrix correspond to an equilibrium state at very low temperature. Both approximations are well satisfied by realistic systems, since the frequencies involved in optical experiments are very high as compared to the device temperature, typically at or below room temperature. As a result, cavity photons can only spontaneously quit the cavity after a lifetime κ^{-1}, while no radiation can enter the cavity from outside.

C. Dissipative emitter dynamics: Losses and pumping

The dissipative dynamics of the emitter requires a bit more care because of the intrinsic nonlinearity of a two-level system. We take each emitter to be independently coupled to its own loss bath with a Hamiltonian of the form

$$H_\gamma = \sum_q (\gamma^*_q S^+ A_q + \gamma_q A^\dagger_q S^-). \tag{10}$$

Here, q indicates the modes of the bath, γ_q, are the coupling constants, and A_q are the bath operators, assumed to have bosonic nature and an initially very low temperature. Performing a Markov approximation, the quantum Langevin equations for the spinlike operators of the emitter read

$$\left.\frac{dS^z}{dt}\right|_\gamma = -\gamma\left(\frac{1}{2} + S^z\right) + G^z_\gamma,$$
$$\left.\frac{dS^+}{dt}\right|_\gamma = \left(i\nu - \frac{\gamma}{2}\right) S^+ + G^+_\gamma. \tag{11}$$

The deterministic part of these equations shows that each emitter tends to decay towards its lower state independently of its neighbors. Differently from what happened to the cavity mode in (8) and (9), the noise operators G^+_γ and G^z_γ now depend on the initial state of the bath $A_q(t_0)$ as well as on the instantaneous spin operators:

$$G^z_\gamma(t) = -i\sum_q [\gamma_q^* e^{-i\omega_q(t-t_0)} S^+(t) A_q(t_0) - \gamma_q e^{i\omega_q(t-t_0)} A_k^\dagger(t_0) S^-(t)], \tag{12}$$

$$G^+_\gamma(t) = -2i\sum_k \gamma_k e^{i\omega_k(t-t_0)} A_k^\dagger(t_0) S^z(t). \tag{13}$$

Under the same conditions assumed for the cavity operators, the quantum noises on the different emitters are uncorrelated and have a delta-like temporal correlation,

$$\langle G^\alpha_{\gamma,i}(t) G^{\alpha'}_{\gamma,j}(t')\rangle = 2D^{\alpha\alpha'}_\gamma(t)\delta(t-t')\,\delta_{ij}. \tag{14}$$

Among the many $\alpha,\alpha' = +, -, z$ terms, the only nonzero diffusion coefficients are

$$D^{-+}_\gamma = \frac{\gamma}{2}, \qquad D^{-z}_\gamma = \frac{\gamma}{2}\langle S^-\rangle, \tag{15}$$

$$D^{z+}_\gamma = \frac{\gamma}{2}\langle S^+\rangle, \quad D^{zz}_\gamma = \frac{\gamma}{2}\left(\frac{1}{2} + \langle S^z\rangle\right). \tag{16}$$

The dependence of the diffusion coefficients on the spin operator averages stems from the intrinsic optical nonlinearity of two-level emitter and makes calculations much harder.

The incoherent external pumping of the system is modeled by coupling each emitter with a bath of inverted oscillators as typically done in laser theory [38]. This leads to quantum Langevin equations of the form

$$\left.\frac{dS^z}{dt}\right|_d = d\left(\frac{1}{2} - S^z\right) + G^z_d, \qquad \left.\frac{dS^+}{dt}\right|_d = \left(i\nu - \frac{d}{2}\right)S^+ + G^+_d. \tag{17}$$

Again, the noise operators G^α_d depend on the spin operators and satisfy delta-like correlation functions in time. The only nonzero diffusion coefficients are now

$$D^{+-}_d = \frac{d}{2}, \quad D^{+z}_d = -\frac{d}{2}\langle S^+\rangle, \tag{18}$$

$$D^{z-}_d = -\frac{d}{2}\langle S^-\rangle, \quad D^{zz}_d = \frac{d}{2}\left(\frac{1}{2} - \langle S^z\rangle\right). \tag{19}$$

Combining the two loss and pumping contributions to the emitter dissipative dynamics, one finally obtains

$$\left.\frac{dS^z}{dt}\right|_{\gamma+d} = \Gamma\left(\frac{\mathcal{D}}{2} - S^z\right) + G^z, \qquad \left.\frac{dS^+}{dt}\right|_{\gamma+d} = \left(i\nu - \frac{\Gamma}{2}\right)S^+ + G^+, \tag{20}$$

where $\Gamma = d+\gamma$ and $G^\alpha(t) = G^\alpha_\gamma(t) + G^\alpha_d(t)$. The stationary value of the average inversion operator S^z in the absence of any cavity field can be called *unsaturated population inversion* and depends only on the ratio between damping rates $x = d/\gamma$,

$$\mathcal{D} = \frac{d-\gamma}{d+\gamma}. \tag{21}$$

In the $\alpha,\alpha' = +, -, z$ basis, the diffusion matrix $D^{\alpha\alpha'}$ of the total external noise operators G^α is given by

$$\begin{pmatrix} 0 & \frac{\gamma}{2} & \frac{\gamma}{2}\langle S^+\rangle \\ \frac{d}{2} & 0 & -\frac{d}{2}\langle S^-\rangle \\ -\frac{d}{2}\langle S^+\rangle & \frac{\gamma}{2}\langle S^-\rangle & \frac{\Gamma}{2}\left(\frac{1}{2} - \mathcal{D}\langle S^z\rangle\right)\end{pmatrix}. \tag{22}$$

D. The quantum Langevin equations

Putting all terms together, we obtain the final quantum Langevin equations for the ith emitter and the $\mathbf{k}$ cavity mode operators,

$$\frac{dS_i^z}{dt} = \Gamma\left(\frac{\mathcal{D}}{2} - S_i^z\right) + \frac{g}{\sqrt{V}}\sum_{\mathbf{k}}(e^{i\mathbf{k}\cdot\mathbf{x}_i} S_i^+ \mathrm{b}_{\mathbf{k}} + e^{-i\mathbf{k}\cdot\mathbf{x}_i}\mathrm{b}^\dagger_{\mathbf{k}} S_i^-) + G_i^z, \tag{23}$$

$$\frac{dS_i^+}{dt} = \left(i\nu - \frac{\Gamma}{2}\right)S_i^+ - \frac{2g}{\sqrt{V}}\sum_{\mathbf{k}} e^{-i\mathbf{k}\cdot\mathbf{x}_i}\mathrm{b}^\dagger_{\mathbf{k}} S_i^z + G_i^+, \tag{24}$$

$$\frac{d\mathrm{b}^\dagger_{\mathbf{k}}}{dt} = \left(i\omega_{\mathbf{k}} - \frac{\kappa}{2}\right)\mathrm{b}^\dagger_{\mathbf{k}} - \frac{g}{\sqrt{V}}\sum_i e^{i\mathbf{k}\cdot\mathbf{x}_i} S_i^+ + F^\dagger_{\mathbf{k}}. \tag{25}$$

These equations can be rewritten in *real space* in terms of field and spin-density operators. Assuming the emitters to be arranged on a regular square lattice with density n_A and to have a fictitious size equal to the lattice cell volume $a = n_A^{-1}$, these latter can be defined as

$$S^\alpha(\mathbf{x}) = \sum_i \delta_a^{(D)}(\mathbf{x} - \mathbf{x}_i)\, S_i^\alpha \tag{26}$$

in terms of delta distributions broadened over a spatial area a. Assuming that the bosonic field $\phi(\mathbf{x})$ is almost constant over a length $\sim a$ allows us to approximate $\delta_a^{(D)}(\mathbf{x})$ as a delta function, simplifying the algebra of the spin densities and the form of the quantum Langevin equations. In this representation, the spin algebra in the Cartesian $\alpha_i = x,y,z$ basis has the form

$$[S^{\alpha_1}(\mathbf{x}), S^{\alpha_2}(\mathbf{x}')] = i\varepsilon_{\alpha_1\alpha_2\alpha_3} S^{\alpha_3}(\mathbf{x})\delta_a^{(D)}(\mathbf{x} - \mathbf{x}'). \tag{27}$$

Summing up, the real-space quantum Langevin equations can be written as

$$\frac{\partial S^z(\mathbf{x})}{\partial t} = \Gamma\left[n_A\frac{\mathcal{D}}{2} - S^z(\mathbf{x})\right] + g[S^+(\mathbf{x})\phi(\mathbf{x}) + \phi^\dagger(\mathbf{x})S^-(\mathbf{x})] + G^z(\mathbf{x}), \tag{28}$$

$$\frac{\partial S^+(\mathbf{x})}{\partial t} = \left[i\nu - \frac{\Gamma}{2}\right]S^+(\mathbf{x}) - 2g\phi^\dagger(\mathbf{x})S^z(\mathbf{x}) + G^+(\mathbf{x}), \tag{29}$$

$$\frac{\partial \phi^\dagger(\mathbf{x})}{\partial t} = \left[i\omega(i\nabla_{\mathbf{x}}) - \frac{\kappa}{2}\right]\phi^\dagger(\mathbf{x}) - gS^+(\mathbf{x}) + F^\dagger(\mathbf{x}), \tag{30}$$

with a spatially local noise correlation

$$\langle G^\alpha(t,\mathbf{x}) G^{\alpha'}(t',\mathbf{x}')\rangle = D^{\alpha\alpha'}(\mathbf{x})\delta_a^{(D)}(\mathbf{x} - \mathbf{x}')\delta(t-t'), \tag{31}$$

with

$$\begin{pmatrix} 0 & \frac{\gamma}{2}\, n_A & \frac{\gamma}{2}\langle S^+(\mathbf{x})\rangle \\ \frac{d}{2}\, n_A & 0 & -\frac{d}{2}\langle S^-(\mathbf{x})\rangle \\ -\frac{d}{2}\langle S^+(\mathbf{x})\rangle & \frac{\gamma}{2}\langle S^-(\mathbf{x})\rangle & \frac{\Gamma}{2}\left(\frac{n_A}{2} - \mathcal{D}\langle S^z(\mathbf{x})\rangle\right) \end{pmatrix}. \tag{32}$$

Another useful representation of the previous equations is in *momentum space*: defining the Fourier transform of the spin density as

$$S^\alpha_{\mathbf{k}} = \int d^d x\, S^\alpha(\mathbf{x}) e^{-i\mathbf{k}\cdot\mathbf{x}}, \quad S^\alpha(\mathbf{x}) = \frac{1}{V}\sum_{\mathbf{k}} S^\alpha_{\mathbf{k}} e^{i\mathbf{k}\cdot\mathbf{x}}, \tag{33}$$

we have the spin commutation relations

$$\left[S^{\alpha_1}_{\mathbf{k}}, S^{\alpha_2}_{\mathbf{k}'}\right] = i\varepsilon_{\alpha_1\alpha_2\alpha_3} S^{\alpha_3}_{\mathbf{k}+\mathbf{k}'}, \tag{34}$$

and the quantum Langevin equations

$$\frac{dS^z_{\mathbf{k}}}{dt} = \Gamma\left(\delta_{\mathbf{k},0} N_A \frac{\mathcal{D}}{2} - S^z_{\mathbf{k}}\right) + \frac{g}{\sqrt{V}}\sum_{\mathbf{q}}(S^+_{\mathbf{k}-\mathbf{q}} \mathrm{b}_{\mathbf{q}} + \mathrm{b}^\dagger_{\mathbf{q}} S^-_{\mathbf{k}+\mathbf{q}}) + G^z_{\mathbf{k}}, \tag{35}$$

$$\frac{dS^+_{\mathbf{k}}}{dt} = \left(i\nu - \frac{\Gamma}{2}\right) S^+_{\mathbf{k}} - 2\frac{g}{\sqrt{V}}\sum_{\mathbf{q}} \mathrm{b}^\dagger_{\mathbf{q}} S^z_{\mathbf{k}+\mathbf{q}} + G^+_{\mathbf{k}}, \tag{36}$$

$$\frac{d\mathrm{b}^\dagger_{\mathbf{k}}}{dt} = \left(i\omega_{\mathbf{k}} - \frac{\kappa}{2}\right)\mathrm{b}^\dagger_{\mathbf{k}} - \frac{g}{\sqrt{V}} S^+_{-\mathbf{k}} + F^\dagger_{\mathbf{k}}. \tag{37}$$

Momentum-space noise operators then satisfy

$$\left\langle G^\alpha_{\mathbf{k}}(t) G^{\alpha'}_{\mathbf{k}'}(t')\right\rangle = 2D^{\alpha\alpha'}_{\mathbf{k}+\mathbf{k}'}\delta(t-t'), \tag{38}$$

with

$$\begin{pmatrix} 0 & \frac{\gamma}{2} N_A \delta_{\mathbf{k},-\mathbf{k}'} & \frac{\gamma}{2}\langle S^+_{\mathbf{k}+\mathbf{k}'}\rangle \\ \frac{d}{2} N_A \delta_{\mathbf{k},-\mathbf{k}'} & 0 & -\frac{d}{2}\langle S^-_{\mathbf{k}+\mathbf{k}'}\rangle \\ -\frac{d}{2}\langle S^+_{\mathbf{k}+\mathbf{k}'}\rangle & \frac{\gamma}{2}\langle S^-_{\mathbf{k}+\mathbf{k}'}\rangle & \frac{\Gamma}{2}\left(\frac{N_A}{2}\delta_{\mathbf{k},-\mathbf{k}'} - \mathcal{D}\langle S^z_{\mathbf{k}+\mathbf{k}'}\rangle\right) \end{pmatrix}. \tag{39}$$

Before proceeding with our discussion, it is worth pointing out that what we have introduced so far is a minimal quantum model to describe condensation in a spatially extended geometry. Depending on the specific system under investigation, other terms might be needed, for instance dephasing of the emitter under the effect of a sort of collisional broadening, or several species of emitters with different resonance frequencies ν_i so to account for more complex gain spectra.

In our formalism, dephasing corresponds to terms of the form

$$\dot\rho = \frac{\Gamma_{\rm coll}}{2}(4S^z\rho S^z - \rho) \tag{40}$$

in the master equation [47], $\Gamma_{\rm coll}$ being the contribution of the dephasing to the dipole relaxation rate. In the quantum Langevin formalism, these processes give additional deterministic terms

$$\left.\frac{dS^+}{dt}\right|_{\rm coll} = -\Gamma_{\rm coll} S^+ + G^+_{\rm coll}, \quad \left.\frac{dS^z}{dt}\right|_{\rm coll} = 0, \tag{41}$$

and an additional contribution to the noise:

$$\begin{aligned} \langle G^+_{\rm coll}(t) G^-_{\rm coll}(t')\rangle &= 2\Gamma_{\rm coll}\left(\tfrac{1}{2} + \langle S^z\rangle\right)\delta(t-t'), \\ \langle G^-_{\rm coll}(t) G^+_{\rm coll}(t')\rangle &= 2\Gamma_{\rm coll}\left(\tfrac{1}{2} - \langle S^z\rangle\right)\delta(t-t'). \end{aligned} \tag{42}$$

We have checked that including such terms does not introduce any qualitatively new feature in the model.

III. MEAN-FIELD THEORY

As a first step in our study of nonequilibrium condensation effects, we study the mean-field solution to the quantum Langevin equations. This amounts to neglecting the quantum noise terms in (35)–(37) and replacing each operator with its expectation value. This study is the simplest in momentum representation, where the mean-field motion equations for $\beta^*_{\mathbf{k}} = \langle \mathrm{b}^\dagger_{\mathbf{k}}\rangle$ and $\sigma^\alpha_{\mathbf{k}} = \langle S^\alpha_{\mathbf{k}}\rangle$ have the form

$$\dot\sigma^z_{\mathbf{k}} = \Gamma\left(\delta_{\mathbf{k},0} N_A \frac{\mathcal{D}}{2} - \sigma^z_{\mathbf{k}}\right) + \frac{g}{\sqrt{V}}\sum_{\mathbf{q}}(\sigma^+_{\mathbf{k}-\mathbf{q}}\beta_{\mathbf{q}} + \beta^*_{\mathbf{q}}\sigma^-_{\mathbf{k}+\mathbf{q}}), \tag{43}$$

$$\dot\sigma^+_{\mathbf{k}} = \left(i\nu - \frac{\Gamma}{2}\right)\sigma^+_{\mathbf{k}} - 2\frac{g}{\sqrt{V}}\sum_{\mathbf{q}}\beta^*_{\mathbf{q}}\sigma^z_{\mathbf{k}+\mathbf{q}}, \tag{44}$$

$$\dot\beta^*_{\mathbf{k}} = \left(i\omega_{\mathbf{k}} - \frac{\kappa}{2}\right)\beta^*_{\mathbf{k}} - \frac{g}{\sqrt{V}}\sigma^+_{-\mathbf{k}} + \frac{i\lambda}{V}\sum_{\mathbf{q}\mathbf{q}'}\beta^*_{\mathbf{q}+\mathbf{q}'}\beta^*_{\mathbf{k}-\mathbf{q}'}\beta_{\mathbf{q}}, \tag{45}$$

very similar to the ones of the semiclassical theory of lasers [48].

A. Stationary state: Bose condensation

While a trivial solution with all $\beta^*_{\mathbf{k}} = \sigma^+_{\mathbf{k}} = 0$ is always present, for some values of the parameters to be specified below, this solution becomes dynamically unstable and is replaced by other *condensed* solutions with a nonvanishing field amplitude. Inspired by experiments, we focus our attention on the case where condensation occurs on the $\mathbf{k} = 0$ state. This corresponds to inserting the ansatz

$$\begin{aligned} \beta^*_{\mathbf{k}}(t) &= \delta_{\mathbf{k}0}\sqrt{V}\,\beta^*_0\, e^{i\omega t}, \\ \sigma^+_{\mathbf{k}}(t) &= \delta_{\mathbf{k}0}\, V\,\sigma^+_0 e^{i\omega t}, \\ \sigma^z_{\mathbf{k}}(t) &= \delta_{\mathbf{k}0}\, V\,\sigma^z_0 \end{aligned} \tag{46}$$

into the mean-field equations, with the amplitudes β^*_0 and σ^+_0, the population inversion σ^z_0, and the frequency ω to be determined in a self-consistent way.

In the $\lambda = 0$ case where direct photon-photon interactions vanish, a direct analytical solution of the mean-field equations gives

$$\omega = \frac{\frac{\nu}{\Gamma} + \frac{\omega_0}{\kappa}}{\frac{1}{\Gamma} + \frac{1}{\kappa}} = \omega_0 + \frac{\kappa}{2}\delta, \tag{47}$$

where $\delta = 2(\nu - \omega_0)/(\Gamma + \kappa)$ is the dimensionless detuning: the frequency ω is therefore equal to an average of the bare field and dipole frequencies, weighted with their bare lifetimes. Analogously, we find for the field and emitter observables

$$|\beta_0|^2 = \frac{\Gamma}{\kappa}\left[n_A \frac{\mathcal{D}}{2} - \frac{\Gamma\kappa}{8g^2}(1+\delta^2)\right], \tag{48}$$

$$\sigma_0^z = \frac{\Gamma\kappa}{8g^2}(1+\delta^2), \tag{49}$$

$$\sigma_0^+ = -\frac{\kappa}{2g}(1+i\delta)\beta_0^*. \tag{50}$$

The condensation threshold is clearly visible in these results: for $\mathcal{D}/\Gamma < \kappa(1+\delta^2)/4g^2 n_A$, the right-hand side of (48) is negative, so only the trivial β_0 solution is possible. For $\mathcal{D}/\Gamma > \kappa(1+\delta^2)/4g^2 n_A$, a condensed solution appears with a finite field intensity (48) and a corresponding emitter dipole moment proportional to (50). We recall that both $\mathcal{D} = (d-\gamma)/(d+\gamma)$ and $\Gamma = d + \gamma = \gamma(1+x)$ are here functions of the pumping rate.

For finite values of λ, a similar derivation can be carried out. For the frequency, it gives

$$\omega = \frac{\frac{\nu}{\Gamma} + \frac{1}{\kappa}(\omega_0 + \lambda|\beta_0|^2)}{\frac{1}{\Gamma} + \frac{1}{\kappa}} = \omega_0 + \lambda|\beta_0|^2 + \frac{\kappa}{2}\delta_\lambda, \tag{51}$$

where the dimensionless detuning $\delta_\lambda = 2(\nu - \omega_0 - \lambda|\beta_0|^2)/(\Gamma + \kappa)$ now involves also the nonlinear frequency shift of the field mode. For the field and the emitter observables, it gives

$$|\beta_0|^2 = \frac{\Gamma}{\kappa}\left[n_A \frac{\mathcal{D}}{2} - \frac{\Gamma\kappa}{8g^2}\left(1+\delta_\lambda^2\right)\right], \tag{52}$$

$$\sigma_0^z = \frac{\Gamma\kappa}{8g^2}\left(1+\delta_\lambda^2\right), \tag{53}$$

$$\sigma_0^+ = -\frac{\kappa}{2g}(1+i\delta_\lambda)\beta_0^*. \tag{54}$$

B. Physical discussion

The most remarkable feature of the mean-field equations is the spontaneous symmetry breaking phenomenon at the condensation threshold. The mean-field equations (43)–(45) are symmetric under the U(1) transformation $(\beta_{\mathbf{k}}^*, \sigma_{\mathbf{k}}^+) \rightarrow (e^{i\varphi}\beta_{\mathbf{k}}^*, e^{i\varphi}\sigma_{\mathbf{k}}^+)$ with arbitrary global phase φ. While for all values of the parameters there is a trivial $\beta_0 = \sigma_0^+ = 0$ solution which fulfills this symmetry, any nontrivial solution has to choose a specific phase for β_0 and σ_0^+, only their modulus being fixed by (48) or (52); as a result, the U(1) symmetry is *spontaneously broken*. In actual experiments, this phase is randomly chosen. Note that since the symmetry transformation does not involve σ_0^z, its mean-field value can always be nonzero.

The behavior of the field intensity $|\beta_0|^2$ and of the oscillation frequency ω is plotted in Fig. 2 as a function of the pumping strength $x = d/\gamma$ for different (negative) values of the natural field-emitter detuning $\nu - \omega_0 < 0$ (different curves) and different values of the (positive) nonlinear coupling $\lambda > 0$ (different panels). In all cases, two thresholds are quite visible: The lower one corresponds to the standard switch-on of laser operation for sufficiently large pump strength. The upper one is a consequence of our specific model and is due to the fact that the gain offered by the emitters is suppressed when the effective emitter linewidth $\Gamma = d + \gamma = \gamma(1+x)$ appearing in (24) is very much broadened by the pumping term d. As usual, whenever a nontrivial $\beta_0 \neq 0$ condensate solution is available, the trivial solution becomes dynamically unstable. For all cases shown in this figure, the order parameter β_0 grows continuously from zero, so the condensation resembles a second-order phase transition.

The behavior of the oscillation frequency shown in the lower panels of Fig. 2 is determined by a complex interplay of the bare frequencies of the cavity and of the emitter, weighted by their respective linewidths and shifted by the nonlinear interaction energy λ according to (51).

The situation for positive detuning $\nu - \omega_0 > 0$ is more complicated and a complete analysis of the rich

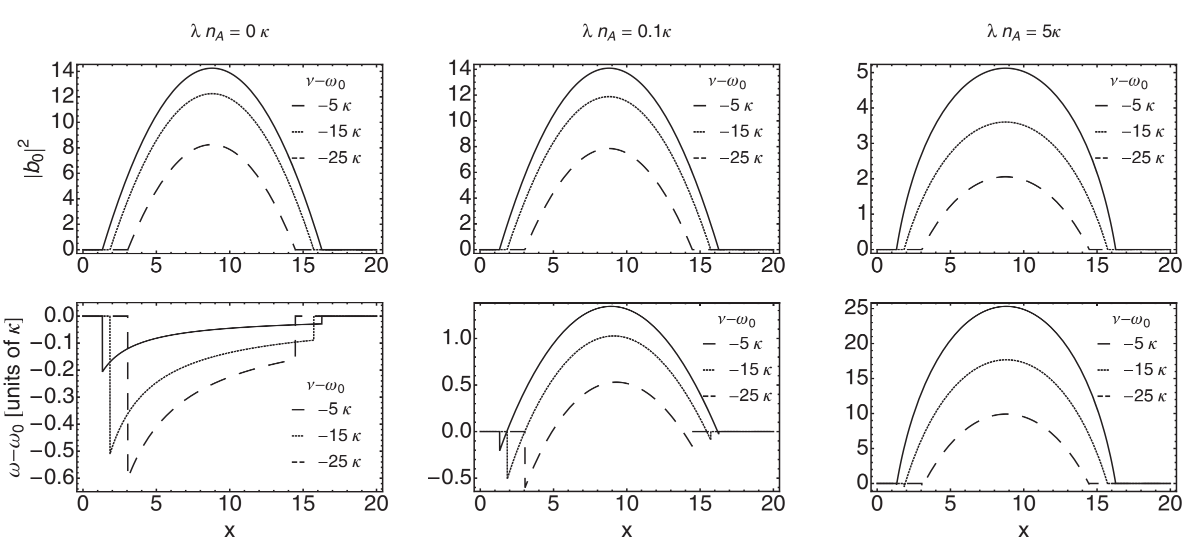

FIG. 2. Intensity of the field (upper panels) and oscillation frequency of the condensate (lower panels) as a function of the pumping parameter $x = d/\gamma$. Both quantities are shown for different values of self-interaction λ and natural detuning $\nu - \omega_0$. In all panels, $\gamma = 10\kappa$ and $g\sqrt{n_A} = 7\kappa$.

phenomenology goes beyond the scope of this work. Not only the order parameter as a function of pumping strength can be discontinuous [49] and bistable, but also the spatial shape of the condensate can develop a complicated structure. As the gain is maximum on a **k**-space ring of modes at a finite k, the choice of the specific combination of modes is determined by complex mechanisms involving the interplay of pumping and dissipation, but also the geometrical details of the system beyond the idealized spatially homogeneous approximation. This complex physics is typical of nonequilibrium systems where no minimal free-energy criterion is available to determine the steady state of the system and is closely related to pattern formation in nonlinear dynamical systems [7]. The first experimental evidence of condensation in spatially nontrivial modes was reported in [17] and discussed in [18]. More complicate spatial features were investigated in [37,50].

IV. QUANTUM FLUCTUATIONS

A. Linearized theory of small fluctuations

The mean-field steady-state solution obtained in the previous section is the starting point for a linearized theory of fluctuations. In the spirit of Bogoliubov and the spin wave approximations, we can linearize Eqs. (35)–(37) around the steady state by performing the operator replacement:

$$\begin{aligned} \mathrm{b}_{\mathbf{k}}^{\dagger} &= (\delta_{\mathbf{k}0}\sqrt{V}\,\beta_0^* + \delta \mathrm{b}_{\mathbf{k}}^{\dagger})e^{i\omega t},\\ S_{\mathbf{k}}^{+} &= (\delta_{\mathbf{k}0}\,V\,\sigma_0^+ + \delta S_{\mathbf{k}}^{+})e^{i\omega t},\\ S_{\mathbf{k}}^{z} &= \delta_{\mathbf{k}0}\,V\,\sigma_0^z + \delta S_{\mathbf{k}}^{z}; \end{aligned} \tag{55}$$

β_0^*, σ_0^+, and σ_0^z are here the mean-field steady states as defined in (52)–(54) with a frequency ω determined by (51). Fluctuations around the mean field are described by the $\delta \mathrm{b}_{\mathbf{k}}^{\dagger}$, $\delta S_{\mathbf{k}}^{+}$, and $\delta S_{\mathbf{k}}^{z}$ operators which inherit the commutation rules from the original $\mathrm{b}_{\mathbf{k}}^{\dagger}$, $S_{\mathbf{k}}^{+}$, and $S_{\mathbf{k}}^{z}$ operators.

Substituting the previous expressions into the motion equations (35)–(37) and neglecting terms of second or higher order in the fluctuation operators, we obtain a set of coupled linear equations

$$\frac{d\mathbf{v}_{\mathbf{k}}}{dt} = \mathbb{A}_{\mathbf{k}}\mathbf{v}_{\mathbf{k}} + \widetilde{\mathbf{F}}_{\mathbf{k}}, \tag{56}$$

for the (rescaled) fluctuation vector

$$\mathbf{v}_{\mathbf{k}}^{t} = \left(\delta\widetilde{\mathrm{b}}_{-\mathbf{k}}^{\dagger},\delta\widetilde{\mathrm{b}}_{\mathbf{k}},\delta S_{\mathbf{k}}^{+},\delta S_{\mathbf{k}}^{-},\delta S_{\mathbf{k}}^{z}\right), \tag{57}$$

with a quantum noise vector

$$\widetilde{\mathbf{F}}_{\mathbf{k}}^{t} = \left(\widetilde{F}_{-\mathbf{k}}^{\dagger},\widetilde{F}_{\mathbf{k}},\widetilde{G}_{\mathbf{k}}^{+},\widetilde{G}_{\mathbf{k}}^{-},\widetilde{G}_{\mathbf{k}}^{z}\right). \tag{58}$$

For notational convenience, we have used the rescaled quantities $\delta\widetilde{\mathrm{b}}_{\mathbf{k}}^{\dagger} = \sqrt{V}\delta \mathrm{b}_{\mathbf{k}}^{\dagger}$ with rescaled noise terms $\widetilde{F}_{\mathbf{k}}^{\dagger} = \sqrt{V}e^{-i\omega t}F_{\mathbf{k}}^{\dagger}$ and $\widetilde{G}_{\mathbf{k}}^{+} = e^{-i\omega t}G_{\mathbf{k}}^{+}$ and $\widetilde{G}_{\mathbf{k}}^{z} = G_{\mathbf{k}}^{z}$. The equations for the Hermitian conjugate quantities $\delta S_{\mathbf{k}}^{-}$ and $\delta \mathrm{b}_{\mathbf{k}}$ follow straightforwardly from $\delta S_{-\mathbf{k}}^{-} = (\delta S_{\mathbf{k}}^{+})^{\dagger}$ and $\delta \mathrm{b}_{\mathbf{k}} = (\delta \mathrm{b}_{-\mathbf{k}}^{\dagger})^{\dagger}$.

Defining the shorthands $z_\lambda = 1 + i\delta_\lambda$ and $\epsilon_{\mathbf{k}} = k^2/2m$, the Bogoliubov matrix $\mathbb{A}_{\mathbf{k}}$ is equal to

$$\mathbb{A}_{\mathbf{k}} = \begin{pmatrix} -\frac{\kappa}{2}z_\lambda + i\epsilon_{\mathbf{k}} + i\lambda|\beta_0|^2 & i\lambda(\beta_0^*)^2 & -g & 0 & 0\\ -i\lambda\beta_0^2 & -\frac{\kappa}{2}z_\lambda^* - i\epsilon_{\mathbf{k}} - i\lambda|\beta_0|^2 & 0 & -g & 0\\ -2g\sigma_0^z & 0 & -\frac{\Gamma}{2}z_\lambda^* & 0 & -2g\beta_0^*\\ 0 & -2g\sigma_0^z & 0 & -\frac{\Gamma}{2}z_\lambda & -2g\beta_0\\ g\sigma_0^- & g\sigma_0^+ & g\beta_0 & g\beta_0^* & -\Gamma \end{pmatrix}. \tag{59}$$

Evaluation of the noise correlation matrix requires a bit more care as the emitter noise depends on the emitter operators themselves. Inserting into (39) the steady-state value of the emitter operators, we have that

$$\left\langle \widetilde{G}_{\mathbf{k}}^{\alpha}\widetilde{G}_{\mathbf{k}'}^{\alpha'}\right\rangle = 2D_{\mathbf{k}+\mathbf{k}'}^{\alpha\alpha'}\,\delta(t-t')\delta_{\mathbf{k}+\mathbf{k}',0} \propto N_A; \tag{60}$$

as in this equation the emitter noise terms $G_{\mathbf{k}}^{\alpha} \propto \sqrt{N_A}$ are of the same order as the other terms in the linearized equations, it is legitimate to replace the spin operators in the diffusion coefficients with their mean-field values. Note that the $\delta_{\mathbf{k}+\mathbf{k}',0}$ coefficient in (60) is a consequence of the assumed ordered arrangement of the emitters: Had we considered a disordered configuration, the zero value for $\mathbf{k}+\mathbf{k}' \neq 0$ would be replaced by something proportional to $\sqrt{N_A}$, still negligible with respect to the value proportional to N_A of the $\mathbf{k}+\mathbf{k}'=0$ term.

The correlation matrix of $\widetilde{\mathbf{F}}_{\mathbf{k}}$ is

$$\langle \widetilde{\mathbf{F}}_{\mathbf{k}}(t)\widetilde{\mathbf{F}}_{\mathbf{k}'}^{\dagger}(t')\rangle = \mathbb{D}\delta(t-t')\delta_{\mathbf{k},\mathbf{k}'} \tag{61}$$

with

$$\mathbb{D} = V\begin{pmatrix} 0 & 0 & 0 & 0 & 0\\ 0 & \kappa & 0 & 0 & 0\\ 0 & 0 & d\,n_A & 0 & -d\sigma_0^+\\ 0 & 0 & 0 & \gamma\,n_A & \gamma\sigma_0^-\\ 0 & 0 & -d\sigma_0^- & \gamma\sigma_0^+ & \Gamma\left(\frac{n_A}{2} - \mathcal{D}\sigma_0^z\right) \end{pmatrix}. \tag{62}$$

As a final remark on the linearization procedure, let us emphasize how our approximations are controlled by the total number of atoms N_A. Assume the scaling

$$S_{\mathbf{k}=0}^{\alpha} \sim N_A, \quad \mathrm{b}_{\mathbf{k}=0} \sim \sqrt{N_A}, \quad D_{\mathbf{k}=0}^{\alpha\alpha'} \sim N_A \tag{63}$$

and

$$S_{\mathbf{k}\neq 0}^{\alpha} \sim \sqrt{N_A}, \quad \mathrm{b}_{\mathbf{k}\neq 0} \sim 1, \quad D_{\mathbf{k}\neq 0}^{\alpha\alpha'} \sim \sqrt{N_A}; \tag{64}$$

together with $g \sim 1/\sqrt{n_A}$ the dependence on N_A of each term in Eqs. (35)–(37) can be made explicit. Then, in the thermodynamical limit $N_A \to +\infty$, retaining the leading order in N_A from such equations is equivalent to performing the mean-field approximation of Sec. III. If the next-to-leading order is also retained, the linearized Bogoliubov theory is recovered.

In analogy with the systematic expansion of equilibrium Bogoliubov theory in powers of the dilution parameter [51], we can make use of these considerations to define a systematic *mean-field* limit for our nonequilibrium system. To this purpose, it is useful to consider the real-space form of the quantum Langevin equations (28)–(30). If we let the atomic density and the photon density $|\phi(\mathbf{x})|^2 \sim S^\alpha(\mathbf{x}) \sim n_A \to \infty$ at constant $g\sqrt{n_A} \sim g|\phi(\mathbf{x})|$ and $\lambda|\phi(\mathbf{x})|^2$, the mean-field equations are not affected [in particular, their steady states (52)–(54)], while the relative importance of the noise terms in the quantum Langevin and of the commutators tends to zero. As a result, the relative magnitude of quantum fluctuation expectation values versus mean-field terms scales as $1/n_A$ in the mean-field limit.

B. The collective Bogoliubov modes

A first step to physically understand the consequences of fluctuations is to study the dispersion of the eigenvalues $\lambda_{\mathbf{k}}^{\mathrm{Bog}}$ of $\mathbb{A}_{\mathbf{k}}$ as a function of k, which gives the generalised Bogoliubov dispersion of excitations on top of the nonequilibrium condensate.

An example of dispersion is shown in Fig. 3: the upper panels show the real part of the dispersion $\mathrm{Re}[\lambda_k^{\mathbf{Bog}}]$ (describing the damping/growth rate of the mode) and the lower panels show the imaginary part $\mathrm{Im}[\lambda_k^{\mathrm{Bog}}]$ (describing the oscillation frequency of the mode). The left column give magnified views of the same dispersion shown on the right column.

As expected there is a Goldstone mode corresponding to the spontaneously broken U(1) symmetry, whose frequency tends to 0 in both real and imaginary parts as $k \to 0$. As typical in nonequilibrium systems [7], this mode is however diffusive rather than sonic; that is, $\mathrm{Im}[\lambda_k^{\mathrm{Bog}}] = 0$ for a finite range around $k = 0$ and the real part starts from zero as $\mathrm{Re}[\lambda_k^{\mathrm{Bog}}] \simeq -\zeta k^2$.

At higher momenta, the diffusive Goldstone mode transform itself into a single-particle cavity photon mode with a parabolic dispersion. Between the two regimes, for $\lambda > 0$ or a finite cavity-emitter detuning δ, there is a sonic-like dispersion of the $\mathrm{Im}[\lambda_k^{\mathrm{Bog}}] \approx c_s|k|$ form (see Fig. 3): for $\lambda > 0$, this is a standard feature of the Bogoliubov dispersion of interacting photons/polaritons [15]. For a finite δ, it follows from the intensity dependence of the refractive index of detuned two-level systems [47]. A connection with the Gross-Pitaevskii formulation of [24] will be given at the end of Sec.V.

In the larger view displayed in the right column, in addition to the Goldstone mode we see two other, almost dispersionless excitation modes. As their origin is mostly due to emitter degrees of freedom, they could not be captured by the Gross-Pitaevskii approach of [24]. Their splitting is related to the Rabi frequency of the optical dressing of the atoms due to the coherent field in the cavity corresponding to the condensate and they are visible in the emitter emission spectrum as the external sidebands of the so-called Mollow triplet of resonance fluorescence [47].

The effect of these additional modes is more evident in Fig. 4, where the chosen parameters are close to a secondary instability. The finite instability wave vector is located at the point where the cavity field dispersion crosses the ones of the dispersionless modes: in this neighborhood, the real part of the dispersion $\mathrm{Re}[\lambda_{\mathbf{k}}^{\mathrm{Bog}}]$ approaches 0 from below. Should $\mathrm{Re}[\lambda_{\mathbf{k}}^{\mathrm{Bog}}]$ go above 0, our ansatz with a uniform condensate localized in the $\mathbf{k} = 0$ mode would no longer be valid and more complicated condensate shapes with spatial modulation should be considered [37,52–54], analogous to secondary instabilities in pattern formation theory [7]. Physically, this *Mollow instability* can be easily interpreted in terms of the well-known optical gain offered by a two-level emitter driven by a strong coherent beam and probed by a weak probe beam detuned by approximately the Rabi frequency of the dressing [47].

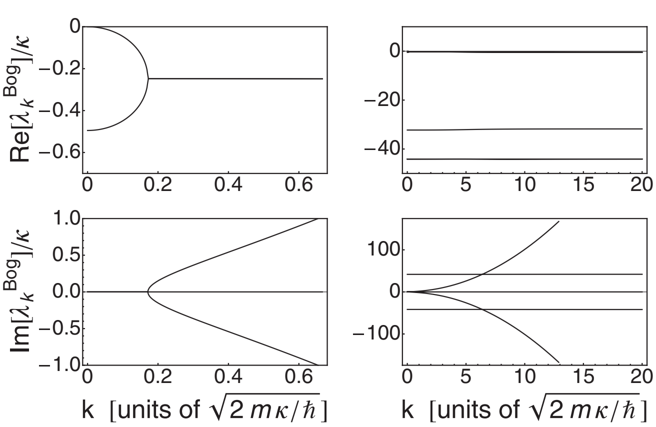

FIG. 3. Dispersion λ_k^{Bog} of the collective modes as predicted by the eigenvalues of the Bogoliubov matrix $\mathbb{A}_{\mathbf{k}}$ in the interacting case with $\lambda n_A = 0.1\kappa$ and $\nu - \omega_0 = -10\kappa$. Left panels show magnified views of the low-$\mathbf{k}$ region of right panels. System parameters: $\gamma = 100\kappa$, $g\sqrt{n_A} = 25$, and $x = 5$.

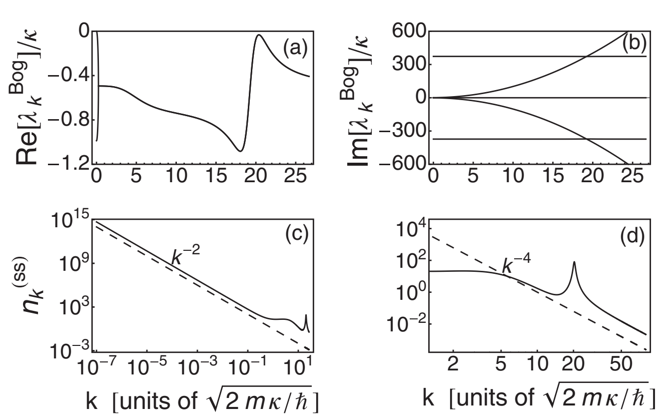

FIG. 4. Imaginary (a) and real (b) part of the dispersion of the collective modes and steady-state momentum distribution (c)–(d) in the vicinity of the Mollow instability onset. (c) shows a magnified view of the low-$\mathbf{k}$ region of (d). System parameters: $\gamma = 10\kappa$, $g\sqrt{n_A} = 42\kappa$, $x = 5$, $\lambda n_A = 0.1\kappa$, $\nu - \omega_0 = 0$.

C. Momentum distribution

From the quantum Langevin equation (56), it is straightforward to extract predictions for one-time physical observables. As a most remarkable example, here we shall concentrate our attention on the steady-state momentum distribution of the cavity field,

$$n^s_{\mathbf{k}} = \langle \mathrm{b}^\dagger_{\mathbf{k}}\, \mathrm{b}_{\mathbf{k}} \rangle = \langle \delta \mathrm{b}^\dagger_{\mathbf{k}}\, \delta \mathrm{b}_{\mathbf{k}} \rangle. \tag{65}$$

On one hand, in contrast to the mean-field approximation where the cavity field is concentrated in the $\mathbf{k} = 0$ mode, this observable is a sensitive probe of fluctuations. On the other hand, it is an experimentally accessible quantity, easily measured from the far-field angular distribution of emitted light. By Fourier transform, it is directly related to the two-point, one-time coherence function of the cavity field, a quantity which is of widespread use in experiments [3,4,31,32].

Grouping in the $\mathbb{V}_{\mathbf{k}} = \langle \mathbf{v}^s_{\mathbf{k}} \mathbf{v}^{s\,\dagger}_{\mathbf{k}} \rangle$ variance matrix the steady-state variances of all operator pairs, from a straightforward integration of the quantum Langevin equations [55], we obtain a Lyapunov equation,

$$\mathbb{A}_{\mathbf{k}} \mathbb{V}_{\mathbf{k}} + \mathbb{V}_{\mathbf{k}} \mathbb{A}^\dagger_{\mathbf{k}} = -\mathbb{D}, \tag{66}$$

from which standard linear algebra methods allow us to extract the variance matrix $\mathbb{V}_{\mathbf{k}}$.

While no simple analytical form is available for $n^s_{\mathbf{k}}$, plots of its behavior are given in the bottom panels of Fig. 5 for several most relevant cases. For small k, the momentum distribution follows the same $1/k^2$ behavior as equilibrium systems provided photons are effectively interacting; that is, either $\lambda > 0$ or $\delta \neq 0$. In the $\lambda = \delta = 0$ case, the situation is more complicated and the distribution appears to diverge as $1/k^4$. Both these results are in agreement with the predictions of the stochastic Gross-Pitaevskii equation in [30]. However, as was noted in [34], great care has to be paid when applying the linearized Bogoliubov-like formalism to low-k modes in nonequilibrium, as the effects beyond linearization can play a dominant role.

At large k, the momentum distribution always decays to zero as $1/k^4$. The large-k decay qualitatively recovers the prediction we guessed in [30] from a phenomenological stochastic Gross-Pitaevskii equation with a frequency-dependent pumping. The specific $1/k^4$ law is a consequence of our choice of monochromatic emitters, whose amplification spectrum decays as $1/(\omega - \nu)^2$; other choices of the emitter distribution would lead to correspondingly different high-momentum tails of $n_{\mathbf{k}}$. The *ab initio* confirmation of this large-k decay of $n_{\mathbf{k}}$ is one of the main results of this article, as it shows that thermal-like momentum distributions can be found also in models where the quasiparticles are not interacting at all and therefore cannot get thermalized by collisional processes. A similar feature was experimentally observed in [20] using a VCSEL device in the weak-coupling regime where photons are practically noninteracting.

The intermediate-k region shows a quite structureless plateau connecting the low-k and high-k regimes. The most interesting feature in this window is the peak that appears at the crossing point of the Goldstone mode and the dispersionless branch when the Mollow instability is approached; see Fig. 6. As usual, the peak height diverges at the onset of the instability.

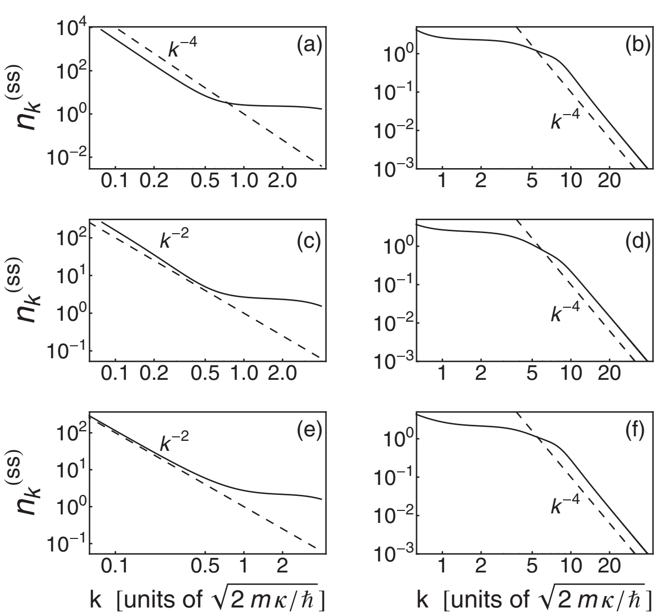

FIG. 5. Steady-state momentum distribution. Left panels show magnified views of the low-$\mathbf{k}$ region of right panels. (a), (b) Noninteracting case $\lambda n_A = \nu - \omega_0 = 0$. (c), (d) $\lambda n_A = 0$, $\nu - \omega_0 = -10\kappa$. (e), (f) $\lambda n_A = 0.1\kappa$, $\nu - \omega_0 = 0$. System parameters: $\gamma = 100\kappa$, $g\sqrt{n_A} = 25$, and $x = 5$.

D. Photoluminescence spectrum

In addition to the one-time observables discussed in the previous section, the quantum Langevin equations also allow for a straightforward evaluation of two-time observables. In particular, we shall concentrate here on the photoluminescence spectrum,

$$S_{\mathbf{k}}(\omega) = \int \frac{dt}{2\pi}\, e^{-i\omega t}\, \langle \mathrm{b}^\dagger_{\mathbf{k}}(t)\, \mathrm{b}_{\mathbf{k}}(0) \rangle, \tag{67}$$

which is accessible from a frequency- and angle-resolved measurement of the emission from the cavity. A detailed study of this quantity in an equilibrium context can be found in [56]. A nonequilibrium calculation using linearized Keldysh techniques was reported in [22].

In our quantum Langevin approach [55], this spectrum is directly obtained as the top-left element of the matrix

$$\mathbb{S}_{\mathbf{k}}(\omega) = \frac{1}{2\pi} (\mathbb{A}_{\mathbf{k}} - i\omega)^{-1} \mathbb{D} (\mathbb{A}^\dagger_{\mathbf{k}} + i\omega)^{-1}; \tag{68}$$

the resonant denominators on the right-hand side of this equation show that the photoluminescence spectrum is peaked along the real part of the Bogoliubov dispersion, while the linewidth of the peaks is set by the imaginary part.

Among the most interesting and nontrivial examples, we show in Fig. 6 the photoluminescence spectrum for two cases of a negative detuning $\delta < 0$ (left) and of finite photon-photon interactions $\lambda > 0$ (right); in both cases, photons are effectively interacting and the Bogoliubov transformation is expected to give spectral weight to the negative "ghost" branch of the Goldstone mode as well [57]. While this feature is clearly visible in the central panel, the effective interaction in the left

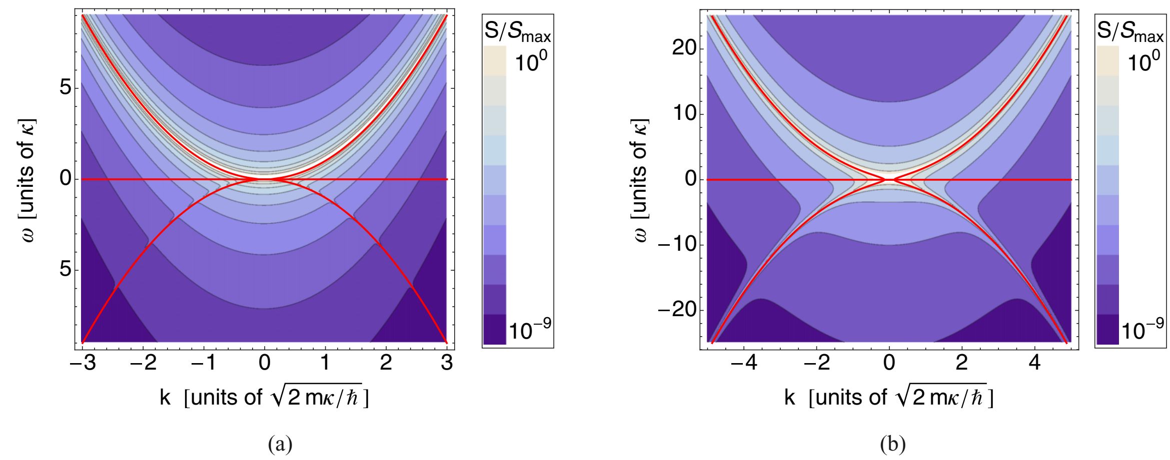

FIG. 6. (Color online) Normalized momentum- and frequency-resolved spectrum of the photoluminescence from the cavity. Left panel: Detuned $\nu - \omega_0 = -35\kappa$ case with $\lambda n_A = 0$. Right panel: Resonant cavity $\nu - \omega_0 = 0$ with photon-photon interactions $\lambda n_A = 0.1\kappa$. Other system parameters: $\gamma = 10\kappa$, $g\sqrt{n_A} = 7\kappa$, $x = 7$.

panel is too weak to give an appreciable effect on this scale: the emitter-cavity detuning that is required for this purpose is in fact much larger than the amplification bandwidth of the emitters and therefore hardly compatible with condensation.

At generic wave vectors and frequencies, the cavity luminescence from the dispersionless branches is typically suppressed by the detuning from the cavity mode. The only exceptions are the crossing points with the cavity mode, where clear peaks can be observed thanks to the resonance of the upper sideband of the Mollow triplet with the cavity mode (not shown).

V. THE STOCHASTIC GROSS-PITAEVSKII EQUATION

In the previous sections we have developed a microscopic model of condensation from which we have obtained predictions for some most interesting observable quantities. In this final section, we are going to discuss how our model can be reduced under suitable approximations to a simpler quantum Langevin equation for the cavity field only. In particular, we shall concentrate on the good-cavity limit $\Gamma/\kappa \gg 1$, where the dynamics of the cavity field occurs on a much faster time scale as compared to the one of the emitters, which can therefore be adiabatically eliminated. Throughout this last section, we will sacrifice mathematical rigor in favor of physical intuition.

A. Adiabatic elimination

Expressing the fields in the rotating frame as

$$\phi^\dagger = \psi^\dagger e^{i\omega t}, \quad S^+ = \mathcal{S}^+ e^{i\omega t}, \quad S^z = \mathcal{S}^z, \tag{69}$$

the real-space equations of motion (28)–(30) can be rewritten as

$$\frac{\partial \mathcal{S}^z}{\partial t} = \Gamma\left(n_A\frac{\mathcal{D}}{2} - \mathcal{S}^z\right) + g(\mathcal{S}^+\psi + \psi^\dagger\mathcal{S}^-) + G^z, \tag{70}$$

$$\frac{\partial \mathcal{S}^+}{\partial t} = -\frac{\Gamma}{2}(1 - i\delta)\mathcal{S}^+ - 2g\,\psi^\dagger\mathcal{S}^z + \widetilde{G}^+, \tag{71}$$

$$\frac{\partial \psi^\dagger}{\partial t} = -\frac{\kappa}{2}(1 + i\delta)\psi^\dagger - i\frac{\nabla^2}{2m}\psi^\dagger - g\mathcal{S}^+ + i\lambda\psi^\dagger\psi^\dagger\psi + \widetilde{F}^\dagger, \tag{72}$$

where $\widetilde{G}^+ = e^{-i\omega t}G^+$ and $\widetilde{F}^\dagger = e^{-i\omega t}F^\dagger$. In the spirit of [58], the limit $\sigma \to +\infty$ can be taken provided that the quantities $g\sqrt{n_A}/\Gamma, \delta, \langle\widetilde{G}^\alpha\widetilde{G}^{\alpha'}\rangle/n_A^2\Gamma^2$ remain finite and that the average $\lambda\langle\psi^\dagger\psi\rangle$ remains negligible with respect to Γ.

While rigorous ways to perform adiabatic elimination for ordinary differential equations exist, the situation is more complicated for our stochastic and quantum case. In what follows we shall then follow a heuristic path inspired from laser theory [40,59] whose validity can be checked *a posteriori* by comparing its predictions with the full model in the linearized case; a brief discussion of a simplified but illustrative example is given in the Appendix. A rigorous derivation of the whole approach is of course needed, but goes far beyond the scope of the present work.

As a first step, we note that time derivatives of the spin densities can be dropped from the equations as they are negligible for large Γ. The spin operators can therefore be expressed in terms of the cavity field using the equations

$$0 = \Gamma\left(n_A\frac{\mathcal{D}}{2} - \mathcal{S}^z\right) + g\left(\mathcal{S}^+\psi + \psi^\dagger\mathcal{S}^-\right) + G^z, \tag{73}$$

$$0 = -\frac{\Gamma}{2}(1 - i\delta)\mathcal{S}^+ - 2g\,\psi^\dagger\mathcal{S}^z + \widetilde{G}^+, \tag{74}$$

$$0 = -\frac{\Gamma}{2}(1 + i\delta)\mathcal{S}^- - 2g\,\mathcal{S}^z\psi + \widetilde{G}^-. \tag{75}$$

From (74) and (75), $\mathcal{S}^+$ and $\mathcal{S}^-$ can be expressed in terms of $\mathcal{S}^z$ as

$$S^+ = \frac{2}{\Gamma(1 - i\delta)}(-2g\psi^\dagger\mathcal{S}^z + \widetilde{G}^+), \tag{76}$$

$$S^- = \frac{2}{\Gamma(1 + i\delta)}(-2g\mathcal{S}^z\psi + \widetilde{G}^-), \tag{77}$$

and hence inserted in (73), which reads

$$\mathcal{S}^z = n_A\frac{\mathcal{D}}{2} - \frac{8g^2}{\Gamma^2(1 + \delta^2)}\psi^\dagger\mathcal{S}^z\psi + \mathbb{G}^z, \tag{78}$$

where

$$\mathbb{G}^z = \frac{2g}{\Gamma^2(1-i\delta)}\widetilde{G}^+\psi + \frac{2g}{\Gamma^2(1+i\delta)}\psi^\dagger\widetilde{G}^- + \frac{1}{\Gamma}G^z. \quad (79)$$

While equal-time spin and cavity operators commute in the full theory, this is no longer true after the elimination, as was noticed in [59]. An ambiguity therefore arises when writing (74) and (75). In the following, inspired by [60], we heuristically propose to choose the generalized normal ordering, $\psi^\dagger\mathcal{S}^+\mathcal{S}^z\mathcal{S}^-\psi$. This issue is important when solving Eq. (78) for $\mathcal{S}^z$, which can be done by formally iterating on $\mathcal{S}^z$:

$$\begin{aligned}\mathcal{S}^z &= n_A\frac{\mathcal{D}}{2}\sum_{m=0}^{+\infty}\frac{(-1)^m}{n_s^m}(\psi^\dagger)^m\psi^m + \sum_{m=0}^{+\infty}\frac{(-1)^m}{n_s^m}(\psi^\dagger)^m\mathbb{G}^z\psi^m\\ &= n_A\frac{\mathcal{D}}{2} : \frac{1}{1+\frac{\psi^\dagger\psi}{n_s}} : + : \frac{1}{1+\frac{\psi^\dagger\psi}{n_s}}\mathbb{G}^z : , \end{aligned} \quad (80)$$

where colons denote normal ordering and the saturation density is defined as

$$n_s = \frac{\Gamma^2}{8g^2}(1+\delta^2). \quad (81)$$

The explicit expression for $\mathcal{S}^z$ can be inserted back in (76) to obtain the expression for $\mathcal{S}^+$ and $\mathcal{S}^-$, which can be finally substituted in (72) to give a quantum stochastic Gross-Pitaevskii equation

$$\begin{aligned}\frac{\partial\psi^\dagger}{\partial t} &= -\frac{\kappa}{2}(1+i\delta)\psi^\dagger - i\frac{\nabla^2}{2m}\psi^\dagger + \psi^\dagger : \frac{P_0(1+i\delta)}{1+\frac{\psi^\dagger\psi}{n_s}} :\\ &\quad + i\lambda\psi^\dagger\psi^\dagger\psi + \mathbb{F}^\dagger,\end{aligned} \quad (82)$$

where the pumping coefficient has the form

$$P_0 = \frac{2g^2 n_A\mathcal{D}}{\Gamma(1+\delta^2)}, \quad (83)$$

and $\mathbb{F}^\dagger$ is a new effective noise operator given by

$$\mathbb{F}^\dagger = \widetilde{F}^\dagger - \frac{2g}{\Gamma(1-i\delta)}\widetilde{G}^+ + \frac{4g^2}{\Gamma(1-i\delta)} : \psi^\dagger\frac{1}{1+\frac{\psi^\dagger\psi}{n_s}}\mathbb{G}^z : . \quad (84)$$

The diffusion matrix of the noise $\mathbb{F}^\dagger$ depends on the field state ψ and $\psi^\dagger$ and can be written in the form

$$\begin{pmatrix}\langle\mathbb{F}^\dagger(\mathbf{x},t)\mathbb{F}(\mathbf{x}',t')\rangle & \langle\mathbb{F}^\dagger(\mathbf{x},t)\mathbb{F}^\dagger(\mathbf{x}',t')\rangle\\ \langle\mathbb{F}(\mathbf{x},t)\mathbb{F}(\mathbf{x}',t')\rangle & \langle\mathbb{F}(\mathbf{x},t)\mathbb{F}^\dagger(\mathbf{x}',t')\rangle\end{pmatrix} = \begin{pmatrix}A & C^*\\ C & B\end{pmatrix}, \quad (85)$$

where A, B, C are functions of ψ and $\psi^\dagger$. Note in particular the nonzero C term in the nondiagonal positions, which originates from the contribution of the emitter noise operators G^α ($\alpha = +,-,z$) to the resulting noise $\mathbb{F}$.

B. Normally ordered c-number representation

A useful technique to obtain physical predictions from the operator-valued stochastic Gross-Pitaevskii equation (82) is to represent it in terms of an equivalent c-number equation. In doing this, we follow the procedure explained in [61]. As one typically does for phase-space representations [38], the first step is to choose an ordering prescription for the operator products according to which all quantities of the theory have to be consistently expressed.

A first choice is to assume normal ordering. In this case, the operator-valued SGPE (82) gets projected onto the c-number Ito SGPE:

$$\begin{aligned}i\,d\psi = \Bigg[&\omega_0 - \frac{\nabla^2}{2m} + \lambda|\psi|^2 + \frac{P_0\delta}{1+\frac{|\psi|^2}{n_s}}\\ &+ i\left(\frac{P_0}{1+\frac{|\psi|^2}{n_s}} - \frac{\kappa}{2}\right)\Bigg]\psi\,dt + dW.\end{aligned} \quad (86)$$

A similar equation was derived in the early theory of laser [11]. The second-order momenta of the noise have local spatial and temporal correlations

$$\langle dW(\mathbf{x},t)dW^*(\mathbf{x}',t)\rangle = 2D_{\psi\psi^*}(\mathbf{x})\,\delta^{(d)}(\mathbf{x}-\mathbf{x}')dt, \quad (87)$$

$$\langle dW(\mathbf{x},t)dW(\mathbf{x}',t)\rangle = 2D_{\psi\psi}(\mathbf{x})\,\delta^{(d)}(\mathbf{x}-\mathbf{x}')dt, \quad (88)$$

and their variances $D_{\psi\psi^*}(\mathbf{x})$ and $D_{\psi\psi}(\mathbf{x})$ depend locally on the field $\psi(\mathbf{x})$. Their value can be determined by imposing that the motion equation for the second moments of the field determined by the c-number equation (86) must be equal to the ones obtained from the operatorial equation (82) in the normal ordered form. Using this prescription, we obtain

$$2D_{\psi\psi^*} = A, \quad 2D_{\psi\psi} = C - \frac{P_0(1-i\delta)}{\left(1+\frac{|\psi|^2}{n_s}\right)^2}\frac{\psi^2}{n_s} - i\lambda\psi^2. \quad (89)$$

As expected from the U(1) symmetry of the original problem, both C and the normal ordering terms in (89) are all proportional to ψ^2. The dependence of the diffusion coefficients on the pumping parameter $x = d/\gamma$ are plotted in Fig. 7 for the mean-field steady state. Remarkably, while $D_{\psi^*\psi}$ and $\mathrm{Re}[D_{\psi\psi}]$ depend very slowly on x and are not much affected by the presence of detuning or self-interaction, the imaginary part $\mathrm{Im}[D_{\psi\psi}]$ crucially depends on these parameters. Note that the possibility of a nonvanishing $D_{\psi\psi}$ variance was overlooked in the phenomenological discussion that we published in [30] and has not been taken into account in [25,33,34].

Due to the saturable pumping term in the SGPE, higher-order momenta of the noise are present beyond the usual Gaussian noise. Their correlation can be extracted by considering the equation of motion for higher-order operator products. Inspired by the so-called truncated Wigner scheme [15,35], one can expect that their contribution is actually negligible in the mean-field limit discussed in Sec. IV.

C. Comparison with full calculation

As a check of the validity of this reformulation, in Fig. 8 we compare the predictions of the SGPE for the dispersion of the collective Bogoliubov modes (upper and central row) and for the momentum distribution (lower row) with the predictions of the full model as derived in Sec. IV.

The Bogoliubov dispersion is obtained by linearizing the deterministic part of the SGPE equation (86) around the steady state. A straightforward calculation gives a dispersion

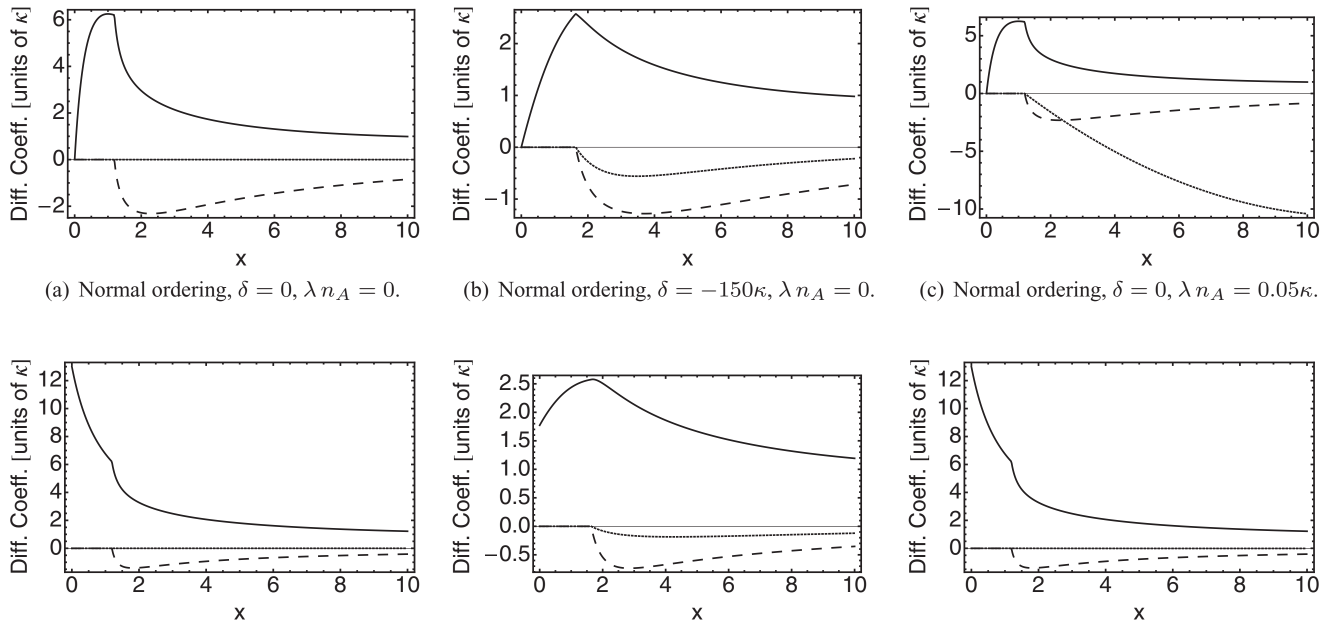

(a) Normal ordering, $\delta = 0$, $\lambda n_A = 0$. (b) Normal ordering, $\delta = -150\kappa$, $\lambda n_A = 0$. (c) Normal ordering, $\delta = 0$, $\lambda n_A = 0.05\kappa$.

(d) Wigner ordering, $\delta = 0$, $\lambda n_A = 0$. (e) Wigner ordering, $\delta = -150\kappa$, $\lambda n_A = 0$. (f) Wigner ordering, $\delta = 0$, $\lambda n_A = 0.05\kappa$.

FIG. 7. Diffusion coefficients $D_{\phi\phi^*}$ (solid lines), Re$[D_{\phi\phi}]$ (dashed lines), and Im$[D_{\phi\phi}]$ (dotted lines) appearing in the SGPE for a field ψ equal to the mean-field steady state. The quantities are plotted as a function of the pumping parameter $x = d/\gamma$ for different regimes of photon-photon interactions (left to right). The top (bottom) row refers to the SGPE in the normal (Wigner) ordering case. In all panels, we have taken $\gamma = 100\kappa$ and $g\sqrt{n_A} = 25\kappa$.

analogous to the one originally obtained in [24],

$$\omega_{\mathbf{k}}^{\pm} = -\Gamma_p \pm \sqrt{\Gamma_p^2 - E_{\mathbf{k}}^2} \tag{90}$$

with the damping parameter $\Gamma_p = \kappa(2P_0 - \kappa)/4P_0$ and the equilibrium Bogoliubov dispersion $E_{\mathbf{k}} = \sqrt{\epsilon_{\mathbf{k}}(\epsilon_{\mathbf{k}} + 2\lambda_{\text{eff}}|\beta_0|^2)}$. In this latter, note that the effective nonlinear term

$$\lambda_{\text{eff}} = \lambda - \frac{\kappa}{2}\frac{\delta}{n_s + |\beta_0|^2} \tag{91}$$

contains two contribution: the former results from the direct photon-photon interaction λ, and the latter describes the

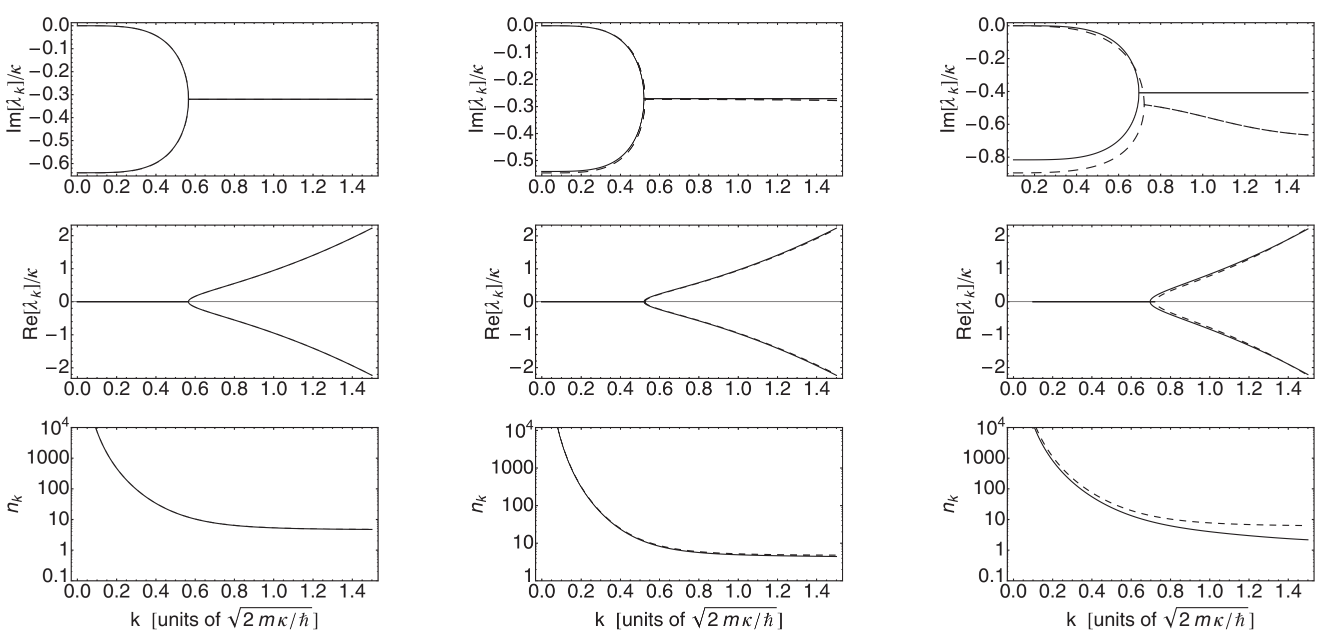

(a) $\gamma = 100\kappa$, $g\sqrt{n_A} = 25\kappa$. (b) $\gamma = 10\kappa$, $g\sqrt{n_A} = 7\kappa$. (c) $\gamma = 1\kappa$, $g\sqrt{n_A} = 2.5\kappa$.

FIG. 8. Comparison between SGPE and the full model. First row and second row: Eigenvalues of the Bogoliubov matrix in functions of the momentum; solid lines refers to SGPE quantities, dashed ones to the full model. Last row: Momentum distributions. In all panels, $\lambda n_A = \nu - \omega_0 = 0$, $x = 2$.

effective Kerr optical nonlinearity due to saturation of the emitters [47].

The momentum distribution shown in the bottom row is instead obtained by reintroducing the noise terms in the linearized equation and then making a small noise expansion: the average of fluctuation operators like $n^s_{\mathbf{k}}$ is written as a linear function of the noise variances $D_{\psi^*\psi}$ and $D_{\psi\psi}$.

In the three columns of Fig. 8, we show the result of the comparison for different system parameters: as one moves deeper in the good-cavity limit (left panels), the agreement becomes very good, while significant discrepancies are expected outside this limit (right panels). As expected, the adiabatic elimination procedure for the momentum distribution is only valid at sufficiently low k when the cavity field detuning is small as compared to the atomic linewidth: breakdown of this condition is indeed visible in the bottom-right panel, where a clear qualitative deviation appears at large k. In particular, the adiabatic elimination of the emitters in the SGPE loses track of frequency dependence amplification and therefore is not able to recover the large k behavior of the momentum distribution. Note also that the quantitative agreement visible in the figure crucially relies on the correct inclusion of the $D_{\psi\psi}$ variance.

In spite of its accurate predictions illustrated in Fig. 8, the stochastic equation (86) is only meaningful at a linearized level. A closer look at the top row of Fig. 7 shows in fact that $|D_{\psi\psi}|$ is not always lower or equal to $D_{\psi\psi^*}$, as is expected from the Cauchy-Schwartz inequality for a generic Ito stochastic equation [55]. While at the linearized level one can forget this fact and formally solve the linear stochastic equation irrespectively on the positivity of the noise variance, this is no longer possible when one wishes to describe the nonlinear dynamics stemming from large fluctuations, e.g., in the vicinity of the critical point for condensation. This feature, often neglected in laser theory [40], is particularly visible in the interacting case for $\lambda \neq 0$ or $\delta \neq 0$. Techniques for numerically solving (generalized) stochastic differential equations with non-positive-definite noise were proposed, the best known example being the so-called positive-P representation which however keeps suffering from other difficulties [38].

D. Symmetrically ordered c-number representation

Another possible way out is to make a different choice for the ordering of operators when performing the projection of the operator-valued SGPE (82) onto the c-number SGPE, e.g., the symmetric ordering of the Wigner representation where c-number averages correspond to symmetrically ordered quantities. In this case, the variance matrix of the noise is indeed positive-definite (see bottom row of Fig. 7), but several other difficulties appear [15,38]. First, the normal ordered saturation term in Eq. (82) cannot be easily symmetrized, which complicates writing of the deterministic part of the stochastic equation. Second, the symmetrization of any nonlinear term in (82) produces terms proportional to the commutator $[\psi(\mathbf{x}),\psi^\dagger(\mathbf{x})]$, which is a UV divergent quantity. Finally, any nonlinear term in (82) will generate a noise with nonvanishing third-order momenta, e.g., $\langle dW^2 dW^*\rangle \propto dt$.

The first two problems can be overcome: the saturation term can be approximated truncating the power expansion to some order, so that symmetrization becomes viable. A finite expression for the field commutator is available if one discretizes the field on a lattice, which corresponds to broadening the delta function according to the smallest accessible length scale of the system. The third problem poses a more challenging task, as noise with such features is extremely difficult to treat. Solutions have been proposed [62,63] but never implemented into the simulation of large systems. Note that this is a well-known issue in the theory of phase-space representation of quantum fields, where interaction terms generate third-order derivatives in the equation for the Wigner function, spoiling its interpretation as a Fokker-Planck equation [38,64]. As already mentioned, truncated-Wigner simulations where these terms are neglected are expected to be correct in the mean-field limit and have been used in simulations of polariton condensation in [35].

VI. CONCLUSIONS

In this article, we have built on laser theory to develop a quantum field model of nonequilibrium Bose-Einstein condensation of photons and polaritons in planar microcavity devices. The system under examination consists of a spatially extended cavity mode coupled to a continuous distribution of externally pumped two-level emitters and is described in terms of quantum Langevin equations. In our view, this is a minimal model that is able to describe nonequilibrium condensation simultaneously including at a quantum level the spatial dynamics of the cavity field, a saturation mechanism, and some frequency dependence of the gain. We expect that such a model may become an essential tool in view of full numerical simulations of the nonequilibrium phase transition.

As a first example of application of our theory, we have worked out the main characteristics of quantum fluctuations around the condensate state. Our calculations confirm the nonequilibrium features that were anticipated by previous theories and/or observed in the experiments: in particular, the collective Bogoliubov modes include a Goldstone branch with diffusive properties, photoluminescence is visible on both upper and lower branches of the Bogoliubov spectrum, and the momentum distribution shows a large-k decrease even in the absence of any collisional thermalization mechanism. This result provides a theoretical explanation to the experimental observation [20] that a condensate can exhibit thermal-like features in the momentum distribution even in the absence of thermalizing collisions. Given the qualitatively different shape of the collective excitation dispersion, we expect that a decisive insight in the equilibrium versus nonequilibrium nature of a condensation process can be obtained by measuring dispersions from the luminescence spectra or via pump-and-probe spectroscopy [16,56,57,65].

In the good-cavity limit, we propose a reformulation of our theory in terms of a stochastic Gross-Pitaevskii equation. In addition to contributing to the justification of a widely used model of nonequilibrium statistical mechanics, this connection allows us to relate the phenomenological parameters of the SGPE to a more fundamental theory. In particular, it turns out that the noise term originates from a complex interplay between pumping and interactions and, in some cases, can even exhibit a multiplicative dependence on the field. This unexpected fact may turn out to have important consequences on the critical properties. To reliably simulate this physics in large systems, further work is needed to overcome subtle issues related to the peculiar statistics of the noise terms.

ACKNOWLEDGMENTS

We are grateful to Andrea Gambassi and Michiel Wouters for continuous stimulating discussions. I.C. acknowledges partial financial support from European Research Council through the QGBE grant and from Provincia Autonoma di Trento.

APPENDIX: ADIABATIC ELIMINATION

In this appendix we will work out a simple example to give a more solid ground to the adiabatic elimination of Sec. V. Let us consider the following simple Ito equations:

$$\begin{aligned} dx &= (-\gamma\, x - g\, y)dt + dW_x, \\ dy &= (-\Gamma\, y - g\, x)dt + dW_y. \end{aligned} \tag{A1}$$

Assuming that one is interested in the slow function $x(t)$ in the limit of $\Gamma \gg \gamma, g$, one can make formally explicit

$$y(t) = -g \int_{-\infty}^{t} dt'\, e^{-\Gamma(t-t')} x(t') + \int_{-\infty}^{t} e^{-\Gamma(t-t')} dW_y(t') \tag{A2}$$

and substitute its expression in the equation for x, to obtain

$$dx = \left[-\gamma x + g^2 \int_{-\infty}^{t} dt'\, e^{-\Gamma(t-t')} x(t')\right] dt + d\widetilde{W}_x, \tag{A3}$$

where we considered the initial time $t_0 = -\infty$ and

$$d\widetilde{W}_x = dW_x - g \int_{-\infty}^{t} e^{-\Gamma(t-t')} dW_y(t'). \tag{A4}$$

Equation (A3) is exact and notice that $d\widetilde{W}_x$ now has a frequency-dependent spectrum. If $\gamma \ll \Gamma$, the kernel $\exp[-\Gamma|t|]$ has a support which is much smaller than the time scale on which $x(t)$ varies appreciably. Therefore one can approximate it as a delta function,

$$\frac{\Gamma}{2} e^{-\Gamma|t|} \simeq \delta(t), \tag{A5}$$

and (A3), (A4) become

$$\begin{aligned} dx &= -\left(\gamma - \frac{g^2}{\Gamma}\right) x\, dt + d\widetilde{W}_x, \\ d\widetilde{W}_x &= dW_x - \frac{g}{\Gamma} dW_y. \end{aligned} \tag{A6}$$

These equations are the same as we would have obtained by simply dropping the temporal derivative dy/dt in (A1), as we did in Sec. V.

[1] R. M. Stevenson, V. N. Astratov, M. S. Skolnick, D. M. Whittaker, M. Emam-Ismail, A. I. Tartakovskii, P. G. Savvidis, J. J. Baumberg, and J. S. Roberts, Phys. Rev. Lett. **85**, 3680 (2000).

[2] J. J. Baumberg, P. G. Savvidis, R. M. Stevenson, A. I. Tartakovskii, M. S. Skolnick, D. M. Whittaker, and J. S. Roberts, Phys. Rev. B **62**, R16247 (2000).

[3] A. Baas, J.-P. Karr, M. Romanelli, A. Bramati, and E. Giacobino, Phys. Rev. Lett. **96**, 176401 (2006).

[4] J. Kasprzak, M. Richard, S. Kundermann, A. Baas, P. Jeambrun, J. Keeling, F. Marchetti, M. Szymanska, R. Andre, J. Staehli, V. Savona, P. Littlewood, B. Deveaud, and L. Dang, Nature (London) **443**, 409 (2006).

[5] J. Klaers, J. Schmitt, F. Vewinger, and M. Weitz, Nature (London) **468**, 545 (2010).

[6] B. Schmittmann and R. K. P. Zia, in *Phase Transitions and Critical Phenomena*, edited by C. Domb and J. L. Lebowitz, Vol. 17 (Academic Press, New York, 1995).

[7] M. C. Cross and P. C. Hohenberg, Rev. Mod. Phys. **65**, 851 (1993).

[8] M. Henkel, H. Hinrichsen, and S. Lbeck, *Non-equilibrium Phase Transitions*, Theoretical and Mathematical Physics (Springer, Berlin, 2009).

[9] R. Graham and H. Haken, Z. Phys. **237**, 31 (1970).

[10] V. DeGiorgio and M. O. Scully, Phys. Rev. A **2**, 1170 (1970).

[11] H. Haken, Rev. Mod. Phys. **47**, 67 (1975).

[12] H. E. Li and K. Iga (eds.), *Vertical-Cavity Surface-Emitting Laser Devices* (Springer Verlag, Berlin, 2003).

[13] C. Chang-Hasnain, IEEE J. Sel. Top. Quantum Electron. **6**, 978 (2000).

[14] L. D. A. Lundeberg, G. P. Lousberg, D. L. Boiko, and E. Kapon, Appl. Phys. Lett. **90**, 021103 (2007).

[15] I. Carusotto and C. Ciuti, Rev. Mod. Phys. **85**, 299 (2013).

[16] M. Wouters and I. Carusotto, Phys. Rev. Lett. **105**, 020602 (2010).

[17] M. Richard, J. Kasprzak, R. Romestain, R. André, and L. S. Dang, Phys. Rev. Lett. **94**, 187401 (2005).

[18] M. Wouters, I. Carusotto, and C. Ciuti, Phys. Rev. B **77**, 115340 (2008).

[19] E. Wertz, L. Ferrier, D. Solnyshkov, R. Johne, D. Sanvitto, A. Lemaître, I. Sagnes, R. Grousson, A. Kavokin, P. Senellart, G. Malpuech, and J. Bloch, Nat. Phys. **6**, 860 (2010).

[20] D. Bajoni, P. Senellart, A. Lemaître, and J. Bloch, Phys. Rev. B **76**, 201305 (2007).

[21] P. Kirton and J. Keeling, Phys. Rev. Lett. **111**, 100404 (2013).

[22] M. H. Szymanska, J. Keeling, and P. B. Littlewood, Phys. Rev. Lett. **96**, 230602 (2006).

[23] M. Wouters and I. Carusotto, Phys. Rev. B **74**, 245316 (2006).

[24] M. Wouters and I. Carusotto, Phys. Rev. Lett. **99**, 140402 (2007).

[25] L. M. Sieberer, S. D. Huber, E. Altman, and S. Diehl, Phys. Rev. Lett. **110**, 195301 (2013).

[26] B. Fischer and R. Weill, Opt. Express **20**, 26704 (2012).

[27] M. Hafezi, P. Adhikari, and J. Taylor, arXiv:1405.5821.

[28] Of course, BEC remains possible if a harmonic trap potential is added to the 2D gas [66], as done in the experiment of [5].

[29] N. D. Mermin and H. Wagner, Phys. Rev. Lett. **17**, 1133 (1966).

[30] A. Chiocchetta and I. Carusotto, Europhys. Lett. **102**, 67007 (2013).
[31] R. Spano, J. Cuadra, G. Tosi, C. Antón, C. A. Lingg, D. Sanvitto, M. D. Martín, L. Viña, P. R. Eastham, M. van der Poel, and J. M. Hvam, New J. Phys. **14**, 075018 (2012).
[32] G. Roumpos, M. Lohse, W. H. Nitsche, J. Keeling, M. H. Szymańska, P. B. Littlewood, A. Löffler, S. Höfling, L. Worschech, A. Forchel, and Y. Yamamoto, Proc. Natl. Acad. Sci. USA **109**, 6467 (2012).
[33] E. Altman, L. M. Sieberer, L. Chen, S. Diehl, and J. Toner, arXiv:1311.0876.
[34] V. Gladilin, K. Ji, and M. Wouters, arXiv:1312.0452.
[35] I. Carusotto and C. Ciuti, Phys. Rev. B **72**, 125335 (2005).
[36] M. Wouters and V. Savona, Phys. Rev. B **79**, 165302 (2009).
[37] J. Keeling and N. G. Berloff, Phys. Rev. Lett. **100**, 250401 (2008).
[38] C. Gardiner and P. Zoller, *Quantum Noise*, 2nd ed. (Springer-Verlag, Berlin, 2000).
[39] M. Lax, Phys. Rev. **145**, 110 (1966).
[40] W. Louisell, *Quantum Statistical Properties of Radiation* (Wiley, New York, 1973).
[41] J. P. Gordon, Phys. Rev. **161**, 367 (1967).
[42] H. Haken, *Laser Theory* (Springer-Verlag, Berlin, 1984).
[43] J. Keeling, F. Marchetti, M. Szymańska, and P. Littlewood, Semicond. Sci. Technol. **22**, R1 (2007).
[44] H. Deng, H. Haug, and Y. Yamamoto, Rev. Mod. Phys. **82**, 1489 (2010).
[45] A.-W. de Leeuw, H. T. C. Stoof, and R. A. Duine, Phys. Rev. A **88**, 033829 (2013).
[46] C. Ciuti and I. Carusotto, Phys. Rev. A **74**, 033811 (2006).
[47] C. Cohen-Tannoudji, J. Dupont-Roc, and G. Grynberg, *Atom-Photon Interactions: Basic Processes and Applications* (Wiley-VCH Verlag GmbH & Co. KGaA, Weinheim, 2004).
[48] M. Scully and M. Zubairy, *Quantum Optics* (Cambridge University Press, Cambridge, 1997).
[49] M. Wouters and I. Carusotto, Phys. Rev. B **75**, 075332 (2007).
[50] G. Christmann, G. Tosi, N. G. Berloff, P. Tsotsis, P. S. Eldridge, Z. Hatzopoulos, P. G. Savvidis, and J. J. Baumberg, Phys. Rev. B **85**, 235303 (2012).
[51] Y. Castin and R. Dum, Phys. Rev. A **57**, 3008 (1998).
[52] D. Sarchi and I. Carusotto, Phys. Rev. B **81**, 075320 (2010).
[53] A. Le Boité, G. Orso, and C. Ciuti, Phys. Rev. Lett. **110**, 233601 (2013).
[54] J. Jin, D. Rossini, R. Fazio, M. Leib, and M. J. Hartmann, Phys. Rev. Lett. **110**, 163605 (2013).
[55] C. Gardiner, *Handbook of Stochastic Methods for Physics, Chemistry and the Natural Sciences*, 3rd ed., Springer Series in Synergetics (Springer-Verlag, Berlin, 2004).
[56] F. M. Marchetti, J. Keeling, M. H. Szymańska, and P. B. Littlewood, Phys. Rev. B **76**, 115326 (2007).
[57] T. Byrnes, T. Horikiri, N. Ishida, M. Fraser, and Y. Yamamoto, Phys. Rev. B **85**, 075130 (2012).
[58] L. A. Lugiato, P. Mandel, and L. M. Narducci, Phys. Rev. A **29**, 1438 (1984).
[59] M. Lax and W. Louisell, IEEE J. Quantum Electron. **3**, 47 (1967).
[60] M. Lax and H. Yuen, Phys. Rev. **172**, 362 (1968).
[61] C. Benkert, M. O. Scully, J. Bergou, L. Davidovich, M. Hillery, and M. Orszag, Phys. Rev. A **41**, 2756 (1990).
[62] L. I. Plimak, M. K. Olsen, M. Fleischhauer, and M. J. Collett, Europhys. Lett. **56**, 372 (2001).
[63] A. Polkovnikov, Phys. Rev. A **68**, 053604 (2003).
[64] K. Vogel and H. Risken, Phys. Rev. A **39**, 4675 (1989).
[65] R. A. Nyman and M. H. Szymańska, Phys. Rev. A **89**, 033844 (2014).
[66] L. Pitaevskii and S. Stringari, *Bose Einstein Condensation* (Clarendon Press, Oxford, 2004).